

Bayesian model reduction

Karl Friston, Thomas Parr and Peter Zeidman

Wellcome Centre for Human Neuroimaging, Institute of Neurology, University College London, UK.

Correspondence: *Peter Zeidman*

The Wellcome Centre for Human Neuroimaging

Institute of Neurology

12 Queen Square, London, UK WC1N 3AR

peter.zeidman@ucl.ac.uk

Abstract

This paper reviews recent developments in statistical structure learning; namely, Bayesian model reduction. Bayesian model reduction is a special but ubiquitous case of Bayesian model comparison that, in the setting of variational Bayes, furnishes an analytic solution for (a lower bound on) model evidence induced by a change in priors. This analytic solution finesses the problem of scoring large model spaces in model comparison or structure learning. This is because each new model can be cast in terms of an alternative set of priors over model parameters. Furthermore, the reduced free energy (i.e., evidence bound on the reduced model) finds an expedient application in hierarchical models, where it plays the role of a summary statistic. In other words, it contains all the necessary information contained in the posterior distributions over parameters of lower levels. In this technical note, we review Bayesian model reduction – in terms of common forms of reduced free energy – and illustrate recent applications in structure learning, hierarchical or empirical Bayes and as a metaphor for neurobiological processes like abductive reasoning and sleep.

Keywords: Bayes methods, biological system modeling, statistical learning

Introduction

Over the past few years, Bayesian model comparison and structure learning have become key issues in the neurosciences [1-6]; particularly, in optimising models of neuroimaging timeseries [7, 8] – and as a fundamental problem that our brains have to solve [9-11]. Indeed, it is often said that the answer to every question is Bayesian model comparison. This joke has, however, a deep truth to it; in the sense that any question – that can be framed in terms of competing hypotheses – can only be answered by appeal to the evidence for those hypotheses. In other words, the answer to any question reduces to a

comparison of hypotheses or model evidence, implicit in the use of Bayes factors, or differences in log evidence [12]. This technical note reviews a relatively new procedure called Bayesian model reduction that has proved useful in both data analysis [13-15] and theoretical neurobiology [9] – to the extent that it is now used routinely in fields such as dynamic causal modelling [16, 17] and active inference. The basic idea behind Bayesian model reduction is straightforward and may find useful applications elsewhere.

To evaluate or score different explanations or models of some data, it is necessary to evaluate their evidence; namely, the probability of sampling some data under a particular model. This involves integrating or marginalising over unknown model parameters, to evaluate the model evidence (also known as the integrated or marginal likelihood). Generally speaking this is an intractable analytic problem that, in many instances, is resolved by maximising a variational (free energy) bound on log evidence [18-22]. This variational free energy is known in machine learning as an evidence lower bound (ELBO). The associated optimisation is known variously as approximate Bayesian inference, variational Bayes and variational ensemble learning, with many special cases such as exact Bayesian inference, variational Laplace, Bayesian (e.g., Kalman) filtering, expectation maximisation, variational message passing, belief propagation, and so on [21-26]. In brief, nearly every (variational) approach to Bayesian model inversion and comparison can be expressed as optimising a variational free energy functional of some data and an approximate posterior distribution or density (denoted herein as Q). The question we focus on is how this variational free energy can be computed quickly and efficiently, under a change of priors – or when adding hierarchical constraints to evaluate a deep or hierarchical model of some data.

In what follows, we briefly review the tenet of variational Bayes, introduce the notion of reduced free energy and review particular forms for continuous and discrete models. The subsequent sections cover applications to model comparison and structure learning, followed by the use of Bayesian model reduction in the inversion of deep or hierarchical models. Both sorts of applications are illustrated with an example from (neuroimaging) data analysis and an application in theoretical neurobiology. These applications are not worked examples; they are taken from the literature to illustrate the sorts of problems that yield to Bayesian model reduction. The accompanying figure legends provide a brief description of the applications (that interested readers can pursue in the original publications).

Bayesian model reduction and reduced free energy

Variational free energy is a functional of some data y and an approximate posterior belief $Q(\theta)$ over the unknown parameters θ of a generative model (i.e., a model of how the data were generated). The free energy has a relatively straightforward form:

$$\begin{aligned}
 F &= E_Q[\underbrace{\ln P(y, \theta)}_{\text{Energy}} - \underbrace{\ln Q(\theta)}_{\text{Entropy}}] \\
 &= \underbrace{\ln P(y)}_{\text{Evidence}} - \underbrace{D_{KL}[Q(\theta_1) \dots Q(\theta_n) \parallel P(\theta | y)]}_{\text{Divergence}} \\
 &= \underbrace{E_Q[\ln P(y | \theta)]}_{\text{Accuracy}} - \underbrace{D_{KL}[Q(\theta_1) \dots Q(\theta_n) \parallel P(\theta)]}_{\text{Complexity}}
 \end{aligned} \tag{1}$$

$$\begin{aligned}
 F &\triangleq F[P(\theta)] \\
 \theta &= (\theta_1, \dots, \theta_n)
 \end{aligned}$$

These expressions show why the evidence lower bound is called free energy. This follows from the fact that free energy can be decomposed it into an *energy* and *entropy* term; namely, the expected log likelihood of some data – under an approximate posterior – and the entropy of that posterior. The rearrangements of this expression show that free energy is log *evidence* minus the Kullback-Leibler divergence between the approximate and true posterior. This means that maximising free energy makes the approximate posterior as close as possible to the true posterior. If the assumed form of the approximate posterior coincides with the true posterior, then we have exact Bayesian inference and the free energy becomes the log evidence. The final rearrangement shows that free energy can also be expressed as *accuracy* minus *complexity*, where complexity is the divergence between the approximate posterior and prior beliefs.

Notice above, that the approximate posterior has been factorised into marginals over a partition of the unknown parameters: $(\theta_1, \dots, \theta_n)$. This is known as a mean field approximation and can greatly simplify model inversion; namely, the maximisation of free energy with respect to the marginal posteriors. Using variational calculus, it is straightforward to show that the approximate posterior of any parameter subset is the expected log probability under its Markov blanket:

$$\begin{aligned}
 \delta_{Q_i} F &= 0 \\
 \Rightarrow \ln Q(\theta_i) &= E_{Q_{\setminus i}}[\ln P(y, \theta)] \approx \ln P(\theta_i | y) \\
 \Rightarrow Q(\theta_i) &= \sigma(E_{Q_{\setminus i}}[\ln P(y, \theta)]) \approx P(\theta_i | y) \\
 \Rightarrow F[P(\theta)] &\approx \ln P(y)
 \end{aligned} \tag{2}$$

Here, σ denotes a softmax function or normalised exponential and $Q \setminus i$ denotes the Markov blanket of the i -th subset [18]. Notice also that we have expressed free energy $F[P(\theta)]$ as a functional of some prior beliefs in Eq. 1. This notation reflects the fact that for any given model or prior belief, a free energy functional of the (approximate) posterior is well defined.

The situation we are concerned with is as follows. Imagine that we have used some approximate Bayesian inference scheme to estimate the parameters of a model – i.e. we have optimised a posterior probability density over the parameters, given prior beliefs and some data. We now want to consider alternative models defined in terms of alternative prior beliefs. Usually, these would constitute reduced models with more precise or informative priors – which constrain or completely eliminate some (mixture of) free parameters. Bayesian model reduction provides a way of evaluating the free energy of the reduced model (i.e., reduced free energy) based on, and only on, the original (full) priors and approximate posteriors. In other words, it allows one to evaluate the evidence for a new set of priors based upon the original estimates; in the same way that classical inference using F tests are based on, and only on, the parameters of a general linear model.

Consider the dual application of Bayes rule to two models defined in terms of the original $P(\theta)$ and reduced $\tilde{P}(\theta)$ priors

$$\frac{\tilde{P}(\theta | y) \tilde{P}(y)}{P(\theta | y) P(y)} = \frac{P(y | \theta) \tilde{P}(\theta)}{P(y | \theta) P(\theta)} \Rightarrow \tilde{P}(\theta | y) = P(\theta | y) \frac{\tilde{P}(\theta) P(y)}{P(\theta) \tilde{P}(y)} \quad (3)$$

Here, we have first expressed Bayes rule with reduced and original priors respectively. We have then re-expressed these as a posterior odds ratio, so that the likelihoods cancel. The last line shows that the posteriors of the reduced model can be expressed in terms of the posteriors of the full model and the ratios of priors and evidences. By integrating over the parameters, we get the evidence ratio of the reduced and full models (where the left hand side of the reduced posterior integrates to unity):

$$\int \tilde{P}(\theta | y) d\theta = 1 = \int P(\theta | y) \frac{\tilde{P}(\theta) P(y)}{P(\theta) \tilde{P}(y)} d\theta \Rightarrow \tilde{P}(y) = P(y) \int P(\theta | y) \frac{\tilde{P}(\theta)}{P(\theta)} d\theta \quad (4)$$

Substituting the approximate values for the model posterior and log evidence from Eq. 2, we get:

$$\begin{aligned}
 \ln \tilde{P}(y) &= \ln \int Q(\theta) \frac{\tilde{P}(\theta)}{P(\theta)} d\theta + \ln P(y) \\
 &\Rightarrow \\
 F[\tilde{P}(\theta)] &\triangleq F[\tilde{P}(\theta) : P(\theta)] \approx \ln E_Q \left[\frac{\tilde{P}(\theta)}{P(\theta)} \right] + F[P(\theta)] \approx \ln \tilde{P}(y) \\
 \ln \tilde{Q}(\theta) &= \ln Q(\theta) + \ln \frac{\tilde{P}(\theta)}{P(\theta)} - \ln E_Q \left[\frac{\tilde{P}(\theta)}{P(\theta)} \right]
 \end{aligned} \tag{5}$$

These (approximate) equalities mean one can evaluate the posterior and evidence of any reduced model, given the posteriors of the full model. In other words, $F[\tilde{P}(\theta) : P(\theta)] \approx \ln \tilde{P}(y)$ allows us to skip the optimization of the reduced posterior $\tilde{Q}(\theta)$ and use the optimised posterior of the full model to compute the evidence (and posterior) of the reduced model directly. Some readers will recognise this as a generalisation of the Savage-Dickey density ratio [27, 28] to any new prior. Furthermore, in the variational setting of approximate Bayesian inference, it is straightforward to evaluate the reduced posterior analytically, because it has been known form (please see examples below).

These computations can be performed rapidly, and may be implemented using the formulae of the next section. As its name implies, Bayesian model reduction can only be used for Bayesian model comparison when all models of interest can be cast as reduced forms of a full model; in other words, the full model must contain all the parameters of any model that will be entertained. This means one cannot compare models that have a completely different form. However, in practice, most model comparisons tend to be framed in terms of models with and without key (sets of) parameters. In what follows, we look at Bayesian model reduction for ubiquitous forms of the approximate posterior for models of continuous and discrete data respectively.

Bayesian model reduction and Variational Laplace

Variational Laplace corresponds to approximate Bayesian inference when assuming the approximate posterior $Q(\theta) = \mathcal{N}(\mu, C)$ is Gaussian. Under this Laplace assumption, the reduced forms of the approximate posterior and free energy have simple forms: see [13] for details.

$$P(\theta) = \mathcal{N}(\eta, \Sigma)$$

$$\tilde{P}(\theta) = \mathcal{N}(\tilde{\eta}, \tilde{\Sigma})$$

$$Q(\theta) = \mathcal{N}(\mu, C)$$

$$\tilde{Q}(\theta) = \mathcal{N}(\tilde{\mu}, \tilde{C})$$

$$\tilde{C}^{-1} = \tilde{P} = P + \tilde{\Pi} - \Pi$$

$$\tilde{\mu} = \tilde{C}(P\mu + \tilde{\Pi}\tilde{\eta} - \Pi\eta)$$

(6)

$$\Delta F = \frac{1}{2} \ln |\tilde{\Pi} P \tilde{C} \Sigma| - \frac{1}{2} (\mu \cdot P\mu + \tilde{\eta} \cdot \tilde{\Pi}\tilde{\eta} - \eta \cdot \Pi\eta - \tilde{\mu} \cdot \tilde{P}\tilde{\mu})$$

$$\Delta F \triangleq F[\tilde{P}(\theta) : P(\theta)] - F[P(\theta)]$$

The last equality defines the change in free energy that corresponds to a variational log Bayes factor. Here Π and Σ are the prior precision and covariance respectively, while P and C are the corresponding posterior precision and covariance. Eq. 6 is derived by substituting Gaussian forms for the probability density functions into Eq. 5; please see [13]. Note that when a parameter is removed from the model, by shrinking its prior variance to zero, the prior and posterior moments become the same and the parameter no longer contributes to the reduced free-energy. Effectively, Eq. 6 allows us to score any reduced model or prior in terms of a reduced free energy, while directly evaluating the posterior over its parameters. The corresponding form for discrete state space models is as follows, when the posteriors and priors have a Dirichlet distribution parameterised in terms of concentration priors.

Bayesian model reduction for discrete models

In the context of models of discrete data, where the posterior has a Dirichlet distribution (and conjugate Dirichlet priors specified in terms of concentration parameters), Bayesian model reduction reduces to something remarkably simple: by applying Bayes rules to full and reduced models it is straightforward to show that the change in free energy (i.e., log Bayes factor) can be expressed in terms of posterior concentration parameters \mathbf{a} , prior concentration parameters \mathbf{a} and the prior concentration parameters that define a reduced or simpler model $\tilde{\mathbf{a}}$. Using $\mathbf{B}(\bullet)$ to denote the beta function, we get [9]:

$$P(\theta) = \text{Dir}(a)$$

$$\tilde{P}(\theta) = \text{Dir}(\tilde{a})$$

$$Q(\theta) = \text{Dir}(\mathbf{a})$$

$$\tilde{Q}(\theta) = \text{Dir}(\tilde{\mathbf{a}})$$

(7)

$$\tilde{\mathbf{a}} = \mathbf{a} + \tilde{a} - a$$

$$\Delta F = \ln B(a) - \ln B(\tilde{a}) + \ln B(\tilde{\mathbf{a}}) - \ln B(\mathbf{a})$$

$$\Delta F \triangleq \Delta F \triangleq F[\tilde{P}(\theta) : P(\theta)] - F[P(\theta)]$$

This equation returns the difference in free energy we would have observed, had we started observing outcomes with simpler prior beliefs. This provides a criterion to accept or reject an alternative hypothesis – or reduced model structure – that is encoded by concentration parameters. For example, if a generative model contains likelihood matrices mapping from discrete (unknown) causes to (known) outcomes, one can parameterise the likelihood mapping with a categorical distribution and a Dirichlet prior. The posterior mapping from causes to outcomes then acquires a Dirichlet form that can be reduced during evidence accumulation. In other words, one can compare models with and without a mapping – between a particular cause and a particular outcome – by evaluating the change in free energy when the corresponding prior concentration parameter is set to zero. This enables a very efficient pruning of redundant parameters in models of discrete state states and outcomes; such as Markov decision processes and hidden Markov models. Intuitively, this form of structure learning enables one to simplify models by removing parameters that reduce the complexity to a greater degree than the implicit loss of accuracy. We will see an example of this below, when applied to modelling how the brain might implement this implicit form of structure learning.

Bayesian model comparison and structure learning

An obvious application of the above expressions is the ‘scoring’ of very large model spaces after inverting a parent model with relatively uninformative (i.e., flat) priors. One can now revisit model assumptions by scoring alternative models in which various combinations of parameters are suppressed or eliminated using precise (i.e., reduced) priors. This enables one to remove redundant parameters and prune models, via the exploration of large model spaces. Fig. 1 & 2 provide an illustration of this application in the context of dynamic causal modelling – the variational inversion of nonlinear state

space models of timeseries data [29]. In this setting, one can evaluate thousands of models in a few seconds. This example uses Gaussian posteriors over continuous states.

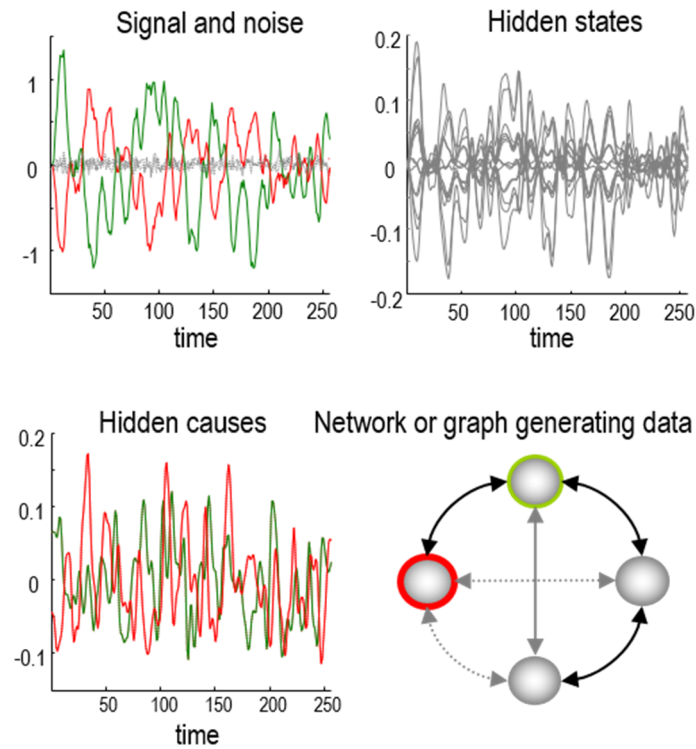


Figure 1: Example of synthetic data used for network discovery in the context of dynamic causal modelling. Upper left panel: simulated data over 256 (3.22 second) time bins comprising signal (solid lines) and correlated observation noise (broken lines). These simulated data were selected from two nodes of a network or graph and were generated as a nonlinear function of node-specific hidden states shown on the upper left. These hidden states evolve dynamically according to equations of motion that model a physiological transduction of neuronal activity into measurable blood flow (hemodynamic) changes in the brain. The (unobserved or hidden) causes of these dynamics are shown on the lower left. These were simply smooth random fluctuations sampled from a Gaussian distribution with a log-precision of eight. Examples of two hidden causes shown here correspond to the two colored regions in the graph (insert on the lower right). This graph depicts four nodes (e.g., brain regions) and all possible edges (putative connections). Hidden causes drive each of the four nodes to produce data. Crucially, the dynamics simulated in each node are communicated to other nodes through bidirectional connections (double headed arrows). When generating synthetic data we chose three out of a maximum of six connections. These are shown as solid arrows. Please see [30] for further details.

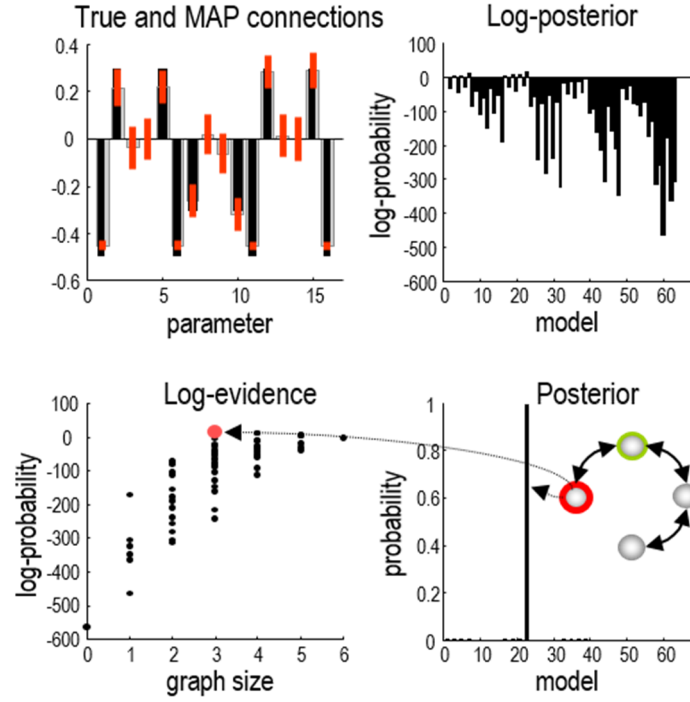


Figure 2: Results of model inversion and Bayesian model reduction, applied to the data of the previous figure. Upper left panel: this shows the conditional means following inversion of a full model of the timeseries data – based upon (stochastic) differential equations modelling network dynamics. The unknown model parameters here correspond to time constants and connectivity within and between four nodes. The resulting posterior means (grey bars) and 90% confidence intervals (red bars) are superimposed on the true values (black bars). It can be seen that – in most instances – the true values fall within 90% confidence (i.e., Bayesian credible) intervals. We have only shown the connections between the nodes in this figure; six of which were zero. Upper right: profile of reduced log-evidences (or log-posterior of each model under flat model priors) over 64 models corresponding to different combinations of connections among the four nodes. Lower left: the same data but plotted as a function of graph size (number of bidirectional) connections. The red dot corresponds to the model with the highest evidence, which was the true model used to generate the data (shown as an inset). Lower right: this portrays the same data as in the corresponding upper panel but after applying a softmax function to create a posterior distribution over the 64 models considered. Please see [14, 30] for further details.

This search removes combinations of parameters that reduce free energy by three or more (i.e., an odds ratio of $\exp(3):1 \approx 20:1$). In this sort of discovery mode, Bayesian model reduction can identify model parameters that entail a complexity cost without a concomitant improvement in model accuracy. The facility for scoring large model spaces is particularly useful in procedures like dynamic causal modelling, where the parameters correspond to the connectivity among the nodes of networks. Clearly, the number of connections and their combinations can become prohibitively large with the size of the network; thereby calling for an efficient model or structure learning scheme. Having scored each model in terms of alternative prior constraints, one can then form Bayesian model averages [31] to provide posterior beliefs about model parameters that properly acknowledge uncertainty about the precise

form or structure of the models entailed. See [14] for details.

Bayesian model reduction in biology

Bayesian model reduction has not only been useful for data analysis and model comparison, it has also been leveraged in the context of computational neuroscience and theoretical neurobiology. Both the elimination of redundant parameters inherent in Bayesian model comparison – and the optimisation of deep, hierarchical models have figured in this context. A nice example of eliminating redundant parameters is sleep; via the elimination or regression of synaptic connections in the brain [32]. This basic notion has been modelled using synthetic (in silico) subjects who have to model contingencies in their world [9]. Using Bayesian model reduction, it is fairly easy to show that simply ‘thinking about things’ off-line can minimise model complexity and lead to much more efficient learning – as illustrated with the example in Fig. 3 & 4. In this example, synthetic subjects were able to enhance their abductive inference (i.e., reasoning), when they engaged Bayesian model reduction after each exposure to sensory data (i.e., feedback). In this illustration, the model space was equipped with extra (hyperprior) constraints that defined the class of models the simulated subjects entertained (here, the class of likelihood mappings between discrete hidden states and observable outcomes). By minimising the complexity of the ensuing models – using Bayesian model reduction – they proved more generalisable to new data and experience; thereby increasing the efficiency of inference and learning. This example used Dirichlet posteriors over discrete states.

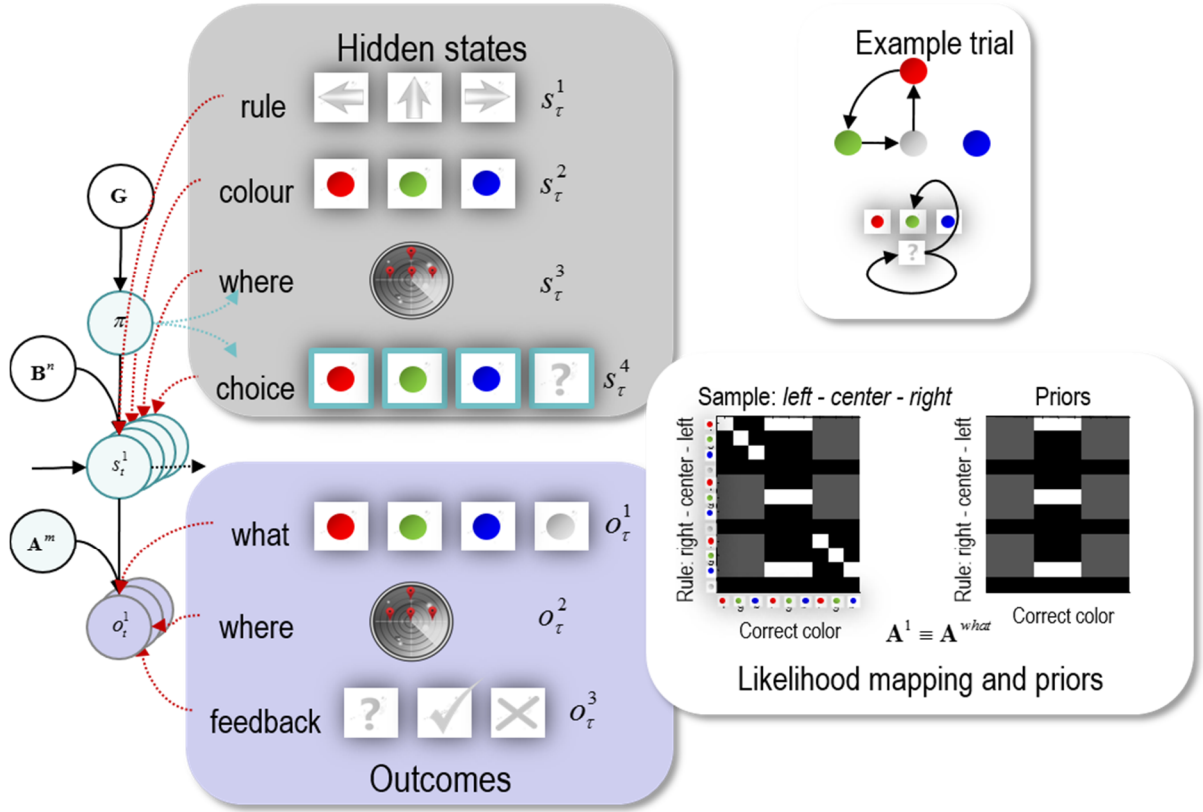


Figure 3: Graphical representation of a generative model used to simulate rule learning. **Left:** The Bayesian network shows the conditional dependencies implied by the generative model. The variables in white circles constitute (hyper) priors, while the blue circles contain random variables. This format shows how outcomes (o) are generated from hidden states (s) that evolve according to probabilistic transitions (B), which depend on policies (π). The probability of a particular policy being selected depends upon its expected free energy (G). The left panels show the particular hidden states and outcome modalities used to simulate rule learning. Here, there are three output modalities comprising coloured visual cues (*what*), proprioceptive cues signalling the direction of gaze (*where*) and (auditory) cues providing feedback (*feedback*). These three sorts of outcomes are generated by the interactions among four hidden states or factors: an abstract rule indicating the location of an informative colour cue (*rule*), the correct colour (*colour*), where attention or saccadic eye movements are directed (*where*) and a (manual) response (*choice*). Hidden states interact to specify outcomes in each modality. In other words, each combination of hidden states has an associated column in the likelihood array (A), which specifies the relative likelihood of outcomes in each modality. For example, if the rule is *left*, the correct colour is red, and the subject is looking at the left cue, the *what* outcome will be *red* and the *where* outcome will be *left*. **Right:** The panel on the upper right shows an example of a trial, where a simulated subject looks from the starting position to the central location, sees a red cue and subsequently looks to the left. After she has seen a green cue she knows the correct colour and returns to the start position, while indicating her choice (*green*). The '?' denotes an undecided choice state (and feedback). The matrices (lower left panel) show the likelihood mapping between hidden states and (*colour*) outcomes assumed, *a priori*, (right) and used to generate actual outcomes (left). These matrices show the likelihood mapping from hidden states to *what* outcomes – the A array for the first or *what* modality. This is a five dimensional array, of which four dimensions are shown under the *undecided* level of the *choice* factor. In other words, these are the contingencies in play until a decision is made. These parameters are shown as a block matrix with 3×3 blocks (*rule* times *where*). Each block shows the 4×3 matrix mapping the correct *colour* to the outcome. Please see Figure 4 for further details.

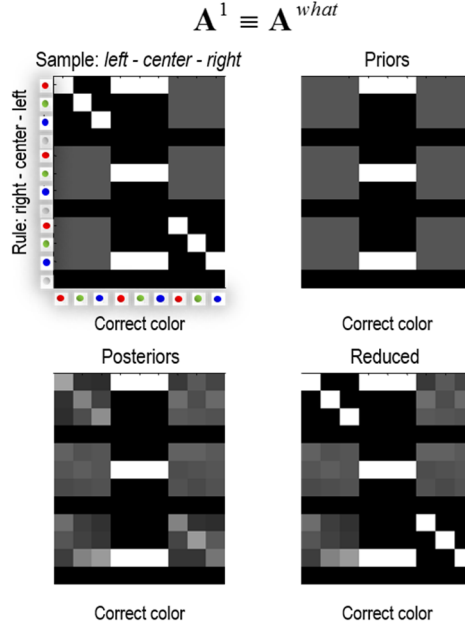


Figure 4: Structure learning: this figure shows the parameters (c.f., connection strengths) that constitute the likelihood mapping from hidden states to *what* outcomes – the \mathbf{A} array for the first modality – parameterised with Dirichlet concentration parameters. This is a five dimensional array, of which four dimensions are shown under the *undecided* level of the *choice* factor. These parameters are shown as a block matrix with 3 x 3 blocks (*rule* times *where*). Each block shows the 4 x 3 matrix mapping the correct *colour* to the outcome. **Upper left:** these represent the true parameters or contingencies. When the synthetic subject is looking at the centre cue (middle column), the rule is uniquely specified by the colour of the outcome. However, when the subject is looking to the left or right (left and right columns), the outcome only depends upon the correct colour if the subject is looking towards the left (when the rule is *left*) or to the right (when the rule is *right*). This context sensitivity is modelled by the diagonal matrices on the upper left and lower right. In all other situations, any colour could be seen. **Upper right:** these are the corresponding expectations of a naive subject. Note that the diagonal matrices have disappeared and there are no beliefs about the relationship between the correct and observed colours. **Lower left:** after 12 trials, the subject has accumulated sufficient experience to acquire knowledge about the (context sensitive) interactions and knows that observed and correct colours predict each other, when and only when looking in the appropriate location. **Lower right:** This knowledge is sufficient to recover the correct contingencies following Bayesian model reduction (c.f., a period of sleep or reflection using Eq. 7). Note the implicit model optimisation removes redundant parameters (connections) between the correct and observed colours; enabling more confident behaviour. Please see [9] for details.

Thus far, we have focused on the use of reduced free energy for model comparison, averaging and selection. In what follows, we now use the same technology to finesse problems in hierarchical, deep or empirical Bayesian models [33].

Hierarchical or deep modelling

In this section, we consider a use of Bayesian model reduction that has proven effective in the inversion of deep or hierarchical models. For example, say one had inverted some highly nonlinear, high-dimensional state space model of several subjects and now wanted to make inferences about model parameters at the between subject level; e.g., [15]. This would necessarily entail some form of hierarchical modelling; however, it would be nice not to have to re-invert each subject-specific model every time some between-subject parameter changed. In this hierarchical setting, the reduced free energy functional above finds a particularly powerful application, because it summarises everything that one needs to know at any level of the hierarchical model, in terms of optimising the approximate posteriors of all levels above. In short, it converts a full hierarchical inversion problem into a succession of Bayesian model reduction problems – in which the posterior beliefs at successively higher levels of the model are optimised based upon the priors and posteriors of the level below.

More formally, consider a hierarchical model expressed in terms of conditional distributions over a succession of unknown model parameters:

$$P(y, \theta) = P(y | \theta_1)P(\theta_1 | \theta_2)P(\theta_2 | \theta_3) \dots P(\theta_n) \quad (8)$$

Imagine now that we inverted the first level of the model, while ignoring any higher constraints from supraordinate levels. We then inverted the first two levels of the model, ignoring third and higher levels – and so on.

$$\begin{aligned} F_1[P(\theta_1)] &= E_{Q_1}[\ln P(y | \theta_1)] - D_{KL}[Q(\theta_1) \| P(\theta_1)] \\ F_2[P(\theta_2)] &= E_{Q_1}[\ln P(y | \theta_1)] - D_{KL}[Q(\theta_1) \| E_{Q_2}[P(\theta_1 | \theta_2)]] - D_{KL}[Q(\theta_2) \| P(\theta_2)] \\ F_3[P(\theta_3)] &= \dots \end{aligned} \quad (9)$$

$$\Rightarrow$$

$$\begin{aligned} F_1[P(\theta_1)] &= E_{Q_1}[\ln P(y | \theta_1)] - D_{KL}[Q(\theta_1) \| P(\theta_1)] \\ F_2[P(\theta_2)] &= F_1[E_{Q_2}[P(\theta_1 | \theta_2)]] - D_{KL}[Q(\theta_2) \| P(\theta_2)] \\ F_3[P(\theta_3)] &= \dots \end{aligned}$$

One can see from the above expressions that the free energy of the full hierarchical model can be expressed recursively in terms of the reduced free energy at all subordinate levels. In other words, as we add hierarchical constraints – with each extra level of the model – the corresponding free energy can be evaluated in terms of the extra complexity incurred at the new level and the reduced free energy

of the previous level under the empirical prior afforded by the new level:

$$\begin{aligned}
 F_i[P(\theta_i)] &= \underbrace{F_{i-1}[E_{Q_i}[P(\theta_{i-1} | \theta_i)]]}_{\text{Accuracy}} - \underbrace{D_{KL}[Q(\theta_i) \| P(\theta_i)]}_{\text{Complexity}} \\
 F_0 &\triangleq \ln P(y | \theta_1) \\
 F_1 &\triangleq F[P(\theta_1)] \\
 F_{i+1}[P(\theta_{i+1})] &\triangleq F[E_{Q_i}[P(\theta_i | \theta_{i+1})] : P(\theta_i)]
 \end{aligned} \tag{10}$$

In this setting, the reduced free energy functional plays the role of an augmented likelihood that has all the necessary information to evaluate the accuracy at any level of the model. This means that we only need to optimise the accuracy (using the free energy functional of posteriors and priors from the lower level) and the complexity due to the parameters at the current level in question.

Heuristically, the use of the reduced free energy functional enables one to replace the sort of analysis used in mixed effects modelling of within and between-subject effects with a summary statistic approach, in a strictly feedforward fashion; i.e., passing sufficient statistics upwards from a lower-level to the next. Here, the reduced free energy functional summarises the evidence for beliefs about parameters at the higher level in terms of the posterior over the parameters of the lower level and the empirical priors from the higher level.

Under Laplace (i.e., Gaussian) or Dirichlet assumptions about the form of the posterior, nothing really changes mathematically when adopting this summary statistic approach. However, the computation times can be greatly improved. This is because one does not have to revisit all lower levels of the hierarchical model to update the posterior beliefs under successive empirical prior afforded by higher levels. Fig. 5 & 6 provide an illustrative example of this approach in the context of dynamic causal modelling. In this example, we were able to estimate experimentally induced changes in brain connectivity that were conserved over subjects. Crucially, the estimation of posterior beliefs over parameters at the between subject level – and ensuing Bayesian model reduction – only took a few seconds; despite the fact that the inversion of each subject’s dynamic causal model could take a minute or so.

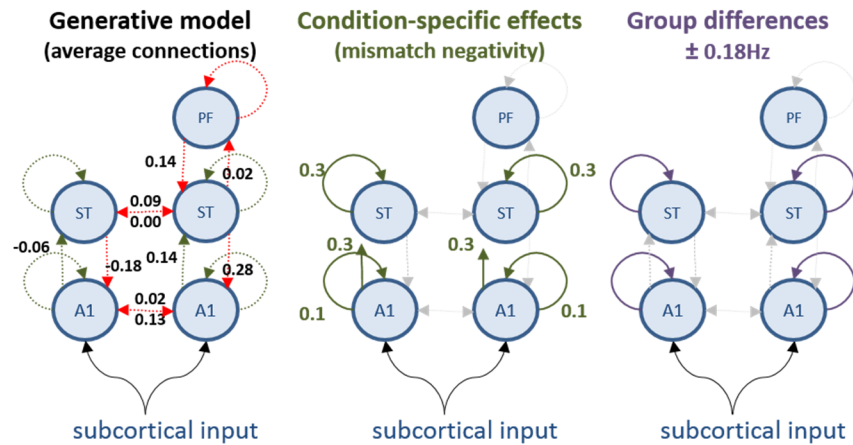


Figure 5: *Simulating electromagnetic responses from multiple subjects.* This figure describes the generative model used to simulate data for subsequent model inversion and reduction (see Figure 2b). The circles represent (electromagnetic) sources of data (recorded by 128 sensors or channels). These sources have intrinsic dynamics, modelled with eight ordinary differential equations per source. The dynamics are perturbed with a parameterised input and coupled to each other through (neuronal) connections. Because the sources are organised hierarchically, one can refer to (between-source or extrinsic) connections as forward or backward. The strengths of these connections correspond to the key model parameters used to generate data from two groups of subjects under two treatment conditions. **Left panel:** The group average connection strengths are shown alongside their connection: red connections do not change with experimental condition, while green connections are equipped with parameters encoding condition-specific effects. The values of the average connectivity over (two) conditions are shown as log scale parameters. **Middle panel:** The strengths of condition-specific differences (within subjects) are labelled in green. These are log scale parameters, where a value of 0.1 corresponds roughly to a scaling of $\exp(0.1) = 1.1$ or 10% increase in coupling. **Right panel:** The solid lines denote the condition-specific effects which differ between two groups of eight subjects. These differences (plus or minus 20% about the average condition-specific effect) are restricted to intrinsic connections at the level of nodes labelled A1 and ST. A1 – primary auditory source; ST – superior temporal source; PF – prefrontal source. Please see [7] for details.

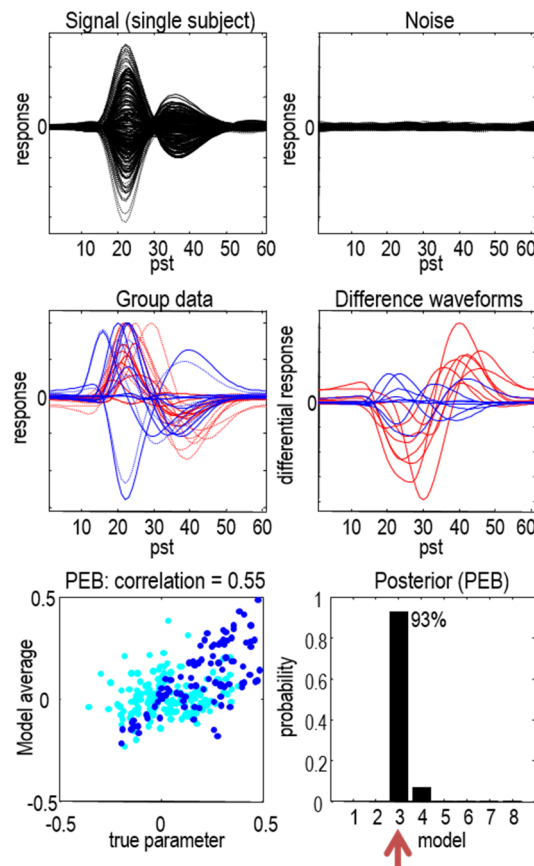


Figure 6: Simulated data and results of Bayesian model reduction using the generative model of the previous figure. The upper panel shows channel data from a single subject as a function of time in (4 ms) time bins. The solid lines (upper left) correspond to the simulated signal, while the dotted lines correspond to signal plus noise. For comparison, the observation noise is shown on the upper right. The middle panels show simulated responses over subjects in terms of a mixture of sensor data. The solid lines (middle left) correspond to the first (*standard*) condition, while the dotted lines report the second (*oddball*) condition for the first group of (*normal*) subjects (red lines) and second group of (*schizophrenic*) subjects (blue lines). The middle right panel shows the condition-specific effects in terms of the waveform differences between the two conditions; namely, a mismatch negativity. It can be seen that this difference is markedly attenuated in the schizophrenic group. This attenuation is mediated by a reduction in the intrinsic connectivity shown in the previous figure. The lower left panel shows the correlation between the estimates of connectivity (cyan dots) and their condition-specific changes (blue dots) with their true values, over all subjects. The lower right panel shows the associated Bayesian model comparison in terms of model likelihoods over eight (within subject) models considered. Bayesian model reduction correctly identifies the third model (red arrow). Please see [7] for details.

Deep (graphical) models in neurobiology

A second example from neurobiology is provided in Fig. 7. Here, this example speaks to the (variational) message passing between levels of a deep or hierarchical model. In this example, a synthetic subject was constructed so that they engaged in a simple form of (iconographic) reading. Crucially, the hierarchical model here involved a separation of temporal scales and a mixture of continuous (lower

level) and discrete (higher-level) states spaces. The communication between the lower (continuous) and higher (discrete) levels of the model used Bayesian model reduction, so that the log evidence for a particular hidden state in the (Markov decision process) model was provided by the free energy lower bound using the reduced free energy. Please see [34, 35] for details.

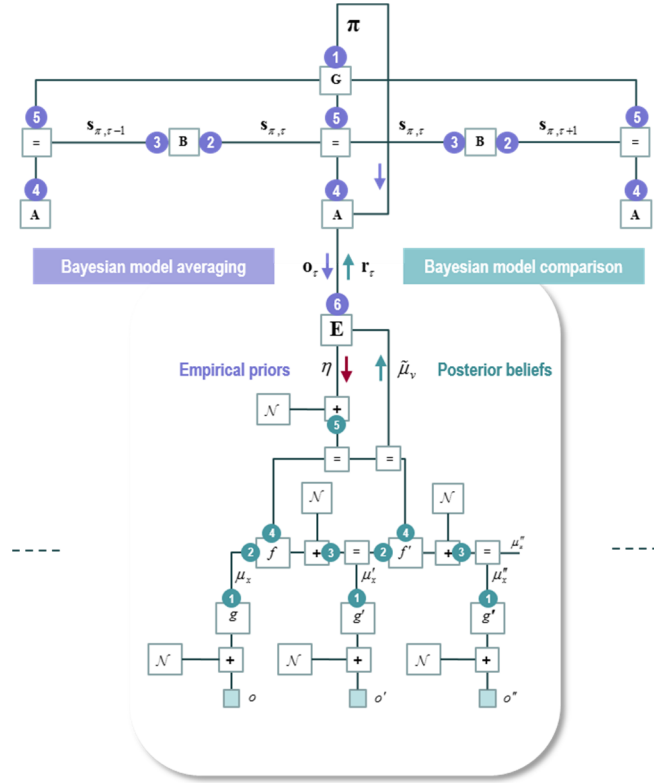


Figure 7: Mixed message passing: this figure uses Forney factor graphs to illustrate a message passing scheme that integrates discrete (Markov decision process) and continuous (state space) models. The upper half of this graph corresponds to a Markov decision process – using the same parameterisation has the generative model in Fig. 3. The key aspect of this message passing scheme is the role of a link node (**E**) associated with the distribution over discrete outcomes – that can also be considered as (outcome) models from the perspective of the (subordinate) continuous level. The consequent message passing means that descending signals from the discrete to continuous levels comprise empirical prior beliefs about the dynamics below, while ascending messages constitute the posterior beliefs over the same set of outcome models. These linking updates entail two sorts of (Bayesian model) averages. First, expected outcomes under each discrete (policy) state are averaged over policy states. Second, prior expectations about causal states are averaged over discrete outcome states. These constitute the descending empirical priors. Conversely, ascending messages correspond to the posterior over outcomes states based upon *Bayesian model reduction*. This treats each discrete causal state as a different model. The expressions in the lower left inset define the log likelihood of continuous observations under each outcome model, relative to the log likelihood under their Bayesian model average. In this example, the continuous model was a state space model whose parameters were determined by the discrete outcome states of the Markov decision process. Please see [34, 35] for details.

Conclusion

In summary, we have reviewed Bayesian model reduction and the free energy functional upon which it rests. This special case of Bayesian model comparison rests upon known, analytic, forms for the prior and posterior densities of any given model. In the setting of approximate Bayesian inference, this usually mandates a variational approach to model fitting, and subsequent comparison. Within this setting – and under the constraint that all interesting models can be specified in terms of prior constraints on a full or parent model – Bayesian model reduction has proven extremely useful. This has been illustrated in terms of structure learning and the Bayesian model comparison over large model spaces. We have then looked at applying the same technology to deep or hierarchical learning, where the reduced free energy provides an efficient summary of the evidence needed to inform beliefs about parameters in successively higher levels. In what follows, we consider instances of Bayesian model reduction in the life sciences; in particular, neurobiology.

In conclusion, we have surveyed the form and applications of reduced free energy in the setting of Bayesian model reduction. Some key areas of application and utility have been highlighted in the hope that the basic ideas could be adopted elsewhere.

Software note

The figures in this note can be reproduced using routines are available as Matlab code in the SPM academic software: <http://www.fil.ion.ucl.ac.uk/spm/>. The simulations in this paper can be reproduced (and customised) via a graphical user interface: by typing >> DEM and selecting the appropriate (e.g., **rule learning**) demo.

Acknowledgements

KJF is funded by the Wellcome Trust (Ref: 088130/Z/09/Z). TP is funded by a Rosetrees Ph.D. Fellowship.

Disclosure statement

The authors have no disclosures or conflict of interest.

References

- [1] M. Zorzi, A. Testolin, and I. P. Stoianov, "Modeling language and cognition with deep unsupervised learning: a tutorial overview," *Front Psychol*, vol. 4, p. 515, 2013.
- [2] D. G. R. Tervo, J. B. Tenenbaum, and S. J. Gershman, "Toward the neural implementation of structure learning," *Curr Opin Neurobiol*, vol. 37, pp. 99-105, Apr 2016.
- [3] J. B. Tenenbaum, C. Kemp, T. L. Griffiths, and N. D. Goodman, "How to grow a mind: statistics, structure, and abstraction," *Science*, vol. 331, pp. 1279-85, Mar 11 2011.
- [4] R. Salakhutdinov, J. B. Tenenbaum, and A. Torralba, "Learning with hierarchical-deep models," *IEEE Trans Pattern Anal Mach Intell*, vol. 35, pp. 1958-71, Aug 2013.
- [5] K. J. Friston, M. Lin, C. D. Frith, G. Pezzulo, J. A. Hobson, and S. Ondobaka, "Active Inference, Curiosity and Insight," *Neural Comput*, vol. 29, pp. 2633-2683, Oct 2017.
- [6] A. G. Collins and M. J. Frank, "Cognitive control over learning: creating, clustering, and generalizing task-set structure," *Psychol Rev*, vol. 120, pp. 190-229, Jan 2013.
- [7] K. Friston, P. Zeidman, and V. Litvak, "Empirical Bayes for DCM: A Group Inversion Scheme," *Front Syst Neurosci*, vol. 9, p. 164, 2015.
- [8] M. W. Woolrich, S. Jbabdi, B. Patenaude, M. Chappell, S. Makni, T. Behrens, *et al.*, "Bayesian analysis of neuroimaging data in FSL," *Neuroimage*, vol. 45, pp. S173-86, Mar 2009.
- [9] K. J. Friston, M. Lin, C. D. Frith, G. Pezzulo, J. A. Hobson, and S. Ondobaka, "Active Inference, Curiosity and Insight," *Neural Comput*, pp. 1-51, Aug 04 2017.
- [10] J. Schmidhuber, "Curious model-building control systems," *In Proc. International Joint Conference on Neural Networks, Singapore. IEEE*, vol. 2, pp. 1458-1463, 1991.
- [11] J. Schmidhuber, "Formal Theory of Creativity, Fun, and Intrinsic Motivation (1990-2010)," *Ieee Transactions on Autonomous Mental Development*, vol. 2, pp. 230-247, Sep 2010.
- [12] R. E. Kass and A. E. Raftery, "Bayes Factors," *Journal of the American Statistical Association*, vol. 90, pp. 773-795, 1995/06/01 1995.
- [13] K. Friston and W. Penny, "Post hoc Bayesian model selection," *Neuroimage* vol. 56, pp. 2089-99, 2011.
- [14] K. J. Friston, V. Litvak, A. Oswal, A. Razi, K. E. Stephan, B. C. van Wijk, *et al.*, "Bayesian model reduction and empirical Bayes for group (DCM) studies," *Neuroimage*, vol. 128, pp. 413-31, Mar 2016.
- [15] V. Litvak, M. Garrido, P. Zeidman, and K. Friston, "Empirical Bayes for Group (DCM) Studies: A Reproducibility Study," *Front Hum Neurosci*, vol. 9, p. 670, 2015.
- [16] S. J. Kiebel, M. I. Garrido, R. Moran, C. C. Chen, and K. J. Friston, "Dynamic causal modeling for EEG and MEG," *Hum Brain Mapp*, vol. 30, pp. 1866-76, Jun 2009.
- [17] K. J. Friston, L. Harrison, and W. Penny, "Dynamic causal modelling," *Neuroimage*, vol. 19, pp. 1273-302, Aug 2003.
- [18] M. J. Beal, "Variational Algorithms for Approximate Bayesian Inference," *PhD. Thesis, University College London*, 2003.
- [19] C. Fox and S. Roberts, "A tutorial on variational Bayes," *Artificial Intelligence Review*, vol. 38, pp. 1-11, 2011.
- [20] D. J. MacKay, "Free-energy minimisation algorithm for decoding and cryptanalysis," *Electronics Letters*, vol. 31, pp. 445-447, 1995.
- [21] F. R. Kschischang, B. J. Frey, and H. A. Loeliger, "Factor graphs and the sum-product algorithm," *IEEE Transactions on Information Theory*, vol. 47, pp. 498-519, 2001.
- [22] J. S. Yedidia, W. T. Freeman, and Y. Weiss, "Constructing free-energy approximations and generalized belief propagation algorithms," *IEEE Transactions on Information Theory*, vol. 51, pp. 2282-2312, Jul 2005.

- [23] S. Mitter and N. Newton, "A variational approach to nonlinear estimation," *SIAM J. Control Optim.*, vol. 42, pp. 1813–33, 2003.
- [24] J. Dauwels, "On Variational Message Passing on Factor Graphs," in *2007 IEEE International Symposium on Information Theory*, 2007, pp. 2546–2550.
- [25] S. Roweis and Z. Ghahramani, "A unifying review of linear gaussian models," *Neural Computation*, vol. 11, pp. 305–345, Feb 1999.
- [26] H.-A. Loeliger, "Least Squares and Kalman Filtering on Forney Graphs," in *Codes, Graphs, and Systems: A Celebration of the Life and Career of G. David Forney, Jr. on the Occasion of his Sixtieth Birthday*, R. E. Blahut and R. Koetter, Eds., ed Boston, MA: Springer US, 2002, pp. 113–135.
- [27] L. J. Savage, *The Foundations of Statistics*. New York: Wiley, 1954.
- [28] I. Verdinelli and L. Wasserman, "Computing Bayes Factors Using a Generalization of the Savage-Dickey Density Ratio," *Journal of the American Statistical Association*, vol. 90, pp. 614–618, 1995.
- [29] J. Daunizeau, O. David, and K. E. Stephan, "Dynamic causal modelling: a critical review of the biophysical and statistical foundations," *Neuroimage*, vol. 58, pp. 312–22, 2011.
- [30] K. J. Friston, B. Li, J. Daunizeau, and K. Stephan, "Network discovery with DCM," *Neuroimage*, vol. 56, pp. 1202–21, 2011.
- [31] N. J. Trujillo-Barreto, E. Aubert-Vazquez, and P. A. Valdes-Sosa, "Bayesian model averaging in EEG/MEG imaging," *Neuroimage*, vol. 21, pp. 1300–19, Apr 2004.
- [32] G. Tononi and C. Cirelli, "Sleep function and synaptic homeostasis," *Sleep Med Rev.*, vol. 10, pp. 49–62, 2006.
- [33] R. E. Kass and D. Steffey, "Approximate Bayesian inference in conditionally independent hierarchical models (parametric empirical Bayes models)," *J Am Stat Assoc.*, vol. 407, pp. 717–26, 1989.
- [34] K. J. Friston, T. Parr, and B. de Vries, "The graphical brain: Belief propagation and active inference," *Network Neuroscience*, vol. 0, pp. 1–34, 2017.
- [35] K. J. Friston, R. Rosch, T. Parr, C. Price, and H. Bowman, "Deep temporal models and active inference," *Neurosci Biobehav Rev*, vol. 77, pp. 388–402, Jun 2017.